Materials Research Proceedings 39 (2024) 9-16 https://doi.org/10.21741/9781644903094-2

Characterization of 316L Stainless Steel Composite Metal Foam Joined by Solid-State Welding Technique

John M. Cance[1] and Afsaneh Rabiei[1, a]

[1] Department of Mechanical and Aerospace Engineering, NCSU, Raleigh, NC 27695, United States

[a]arabiei@ncsu.edu

Keywords: Composite Metal Foam, Solid-State Welding, Microstructure, Mechanical Properties

Abstract. In previous studies, composite metal foams (CMF) have shown exemplary mechanical performance under impact which has made them prime candidates for protection of transported passengers and cargo. [1] Materials utilized in such applications often require joining to form structures and geometries that are far more complex or impossible to produce in an as-manufactured state. Welding methods are popular in the joining of metals with solid-state welding processes such as induction welding being of particular interest in the studies to be discussed. In this study, various thicknesses of 316L stainless steel CMF are manufactured through powder metallurgy technique and welded using Induction Welding. The mechanical properties of the weldments were studied through uniaxial tensile tests while microstructural characterization of the weldment within the joint interface and heat-affected zone (HAZ) are evaluated using scanning electron microscopy. The combination of these evaluations grant insight on the effects of various weld parameters (e.g., welding temperature, workpiece thickness, flux, and welding environment) as well as the suitability and restrictions of induction welding in the joining of 316L Stainless Steel CMF.

1. Introduction

The industrialized structure of first-world countries has steadily necessitated a heightened volume of resources to be transported domestically through roads and railways in recent decades. Railways in particular account for almost half of the freight transported within the United States with unparalleled fuel efficiency. However, roughly 75% of this content consists of hazardous materials (HAZMAT) which, while necessary in forms such as fuels and chemicals, can harbor catastrophic results when introduced to the environment through tank car derailment and subsequent rupture. [2,3] One such scenario came to fruition in 2013 when 72 DOT-111 tank cars containing crude oil derailed in Lac-Mégantic, Quebec, Canada, resulting in fires that claimed 47 lives and destroyed much of the local infrastructure. [4] This tragedy resulted in the development of DOT-117 and DOT-117R standard tank cars, bolstered for HAZMAT transport by a layer of fire-retardant insulation as well as welded external jackets and head shields of TC-128B steel to dampen impact in the event of derailment. However, advancement is still pursued in this field to further improve durability of tank cars transporting HAZMAT and subvert potential tragedies caused by loss of lading.

Metal foams are unique family of materials characterized by their low-density porous structures and high strength-to-weight ratio, allowing impressive degrees of thermal insulation and impact energy absorption. [5] This performance has led to metal foams gaining preference in the automotive and aerospace industries to further improve user safety in the event of impact while simultaneously facilitating development of lightweight components. However, conventional metal foams are often mechanically unpredictable, due to their nonuniform porosity sizes, profiles, and distribution within the product. Under compressive loading, this can result in formation of

collapse bands as larger cells implode, leading to a premature failure of the material with low energy absorption capacity. [5,6] Steel-steel composite metal foam (S-S CMF) has been shown to circumvent this effect by forgoing the traditionally foamed closed cells in favor of similar hollow 316L steel spheres surrounded by a sintered 316L steel matrix. This allows the cells to distribute compressive load with relative homogeneity while bonding between the matrix and outer sphere walls provides additional support, resulting in superior mechanical performance compared to conventional metal foams.[1]

Construction of large structures such as plane fuselages and railcars is heavily reliant on welding of constituent materials, such as metal sheets and panels. Despite the joining of bulk metals being widely explored, unique concerns are presented when determining suitable processes for welding porous metals. The most pressing one being preservation of the cellular structure, and its inherent benefits, without sacrificing integrity of the welded joint. Because of this, fusion welding methods are often overlooked as their propensity to liquify the bonded interface results in a weld more akin to a bulk material upon solidification, exacerbating the already present concern of inhomogeneous behavior. Conversely, solid-state welding methods have relatively minimal effects on the base material, substituting the intensity of a direct arc/flame in favor of induction or frictional heating combined with external pressure to encourage the mating of the bonding surfaces. Induction welding is of particular interest in this study. Induction coils were used to induce Eddy currents within the workpiece and set bonding temperatures were achieved through resistance between the induced current and workpieces. This results in a solid weld while minimizing heat effects on the material, making induction welding a suitable option for joining S-S CMF panels. In this study, the properties of S-S CMF panels of various thicknesses joined using induction welding will be presented and the benefits and limitations of this solid-state joining will be discussed.

2. Experimental

2.1 Materials and processing

The S-S CMF panels welded in this study were manufactured through the powder metallurgy (PM) method established in previous publications [7]. The 316 stainless steel hollow spheres with average outer diameters of 2mm and wall thickness of 0.1mm were used (produced by Hollomet GmbH located in Dresden, Germany). Additionally, matrix material was comprised of 316L stainless steel powder atomized by North American Höganäs High Alloys LLC. The resulting S-S CMF panels ranged in density from 2.5 to 3.3g/cc. The sintering process was followed by sectioning of the panels into rectangular workpieces using waterjet cutting. These reduced panels were then brought to final dimensions through facing and end milling. Final thicknesses were modified within a range of 10.2mm to 28.32mm to observe the influence of panel thickness on penetration of Eddy current during the induction welding process. In preparation for welding, intended bonding surfaces underwent additional milling and grinding to provide an even finish.

All induction welding of the S-S CMF panels was conducted by Advanced Materials Manufacturing (AMM), a startup company based in Raleigh, NC. An ECO-LINE MFG 100 and ECO-LINE MFG 500 high-frequency power sources from Eldec was used for this purpose. Two induction coil designs were used for both groups, interchanged based on panel thickness. Both designs possessed a C-shaped profile outfitted with rectangular ferrotrons along the length to facilitate a more uniform heating profile on the top and bottom of the welding panels, as well as along the interface length. Panels of S-S CMF were paired for joining based on corresponding thicknesses to avoid significant distortion at the weld and achieve consistent bonding. Both coils featured even distributions of ferrotrons along the top and bottom, with Coil #1 possessing a 20-27mm wide opening to accommodate thinner panels while Coil #2 enveloped thicker panels with a 40mm gap. Overall, the welding procedure was relatively similar throughout the selected pairs

of CMF panels (shown in Table 1). Each set was fastened within a vise, maintaining contact between the workpieces as they were heated by the induction coil, before cooling and removal. Welding temperatures were determined for each sample set using a FLIR infrared camera directed at the joint interface. This general arrangement of the induction welding process is shown below in Fig. 1, where the heated joint between CMF panels is highlighted in red. Despite these similarities, group 1 weld surface preparation was conducted using a mixture of water and Royal Tiger flux applied to the mating surfaces prior to welding. In this stage, all samples were welded in air. Conversely, group 2 omitted the water base flux to eliminate some oxidation issues. Additional runs were conducted in argon to minimize oxidation. These combined efforts resulted in welded S-S CMF panels with solid contact along the bonded interface and a surface relatively free of visible defects, as Shown in Fig. 2.

Table 1. Induction welded panels arranged by applied welding parameters.

Group	Thickness [mm]	Weld Temp [°C]	Environment	Flux
1	10.2	1220	Air	Yes
	15.2	969	Air	Yes
	17.7	1100	Air	Yes
	22.5	850	Air	Yes
2	21.2	1050	Argon	No
	26.39	1100	Air	No
	28.32	1070	Argon	No

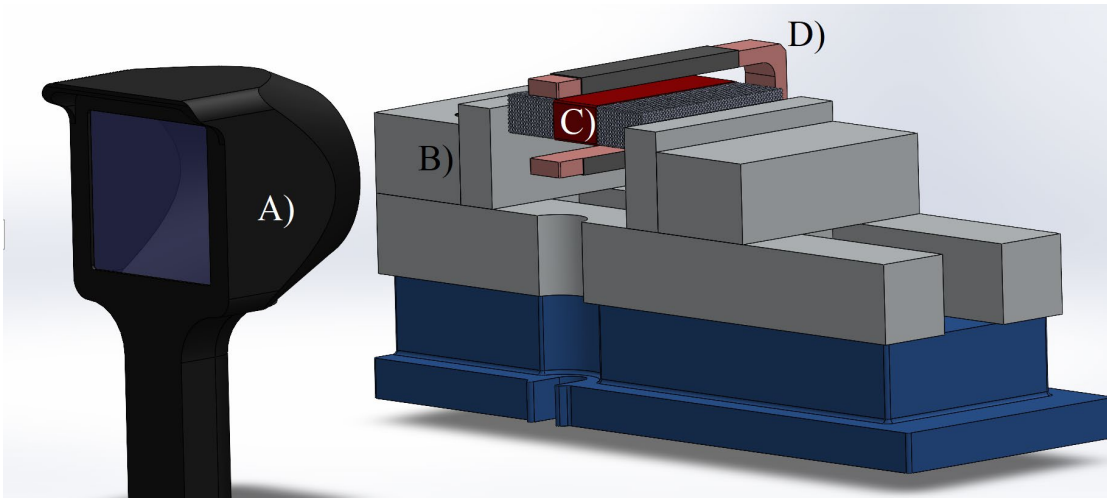

Fig. 1. Recreation of the induction welding setup consisting of A) the FLIR IR camera, B) vise, C) abutted S-S CMF panels, and D) an induction coil outfitted with ferrotrons, displayed as solid dark grey regions.

Materials Research Proceedings 39 (2024) 9-16 https://doi.org/10.21741/9781644903094-2

Induction welding was followed by face milling to remove surface features that may affect tensile performance at the weld seam. Tensile specimens of the induction welded panels were designed based on AWS B4.0:2016 standards for transverse rectangular tensile test and extracted from the welded plates. Due to the varied sizing of welded panels produced, scaling was required to accomodate 2 to 3 tensile specimens per weld, allowing thorough mechanical characterization along the seam. Test specimens for group 1 were extracted through waterjet cutting then ground along the cut surfaces to remove any resulting imperfections, while group 2 panels were sectioned using a band saw and brought to their final profiles through end milling. A schematic of the tensile specimen arrangements along a pair of welded panels is shown below in Fig. 3, where the weld line is represented by a red line.

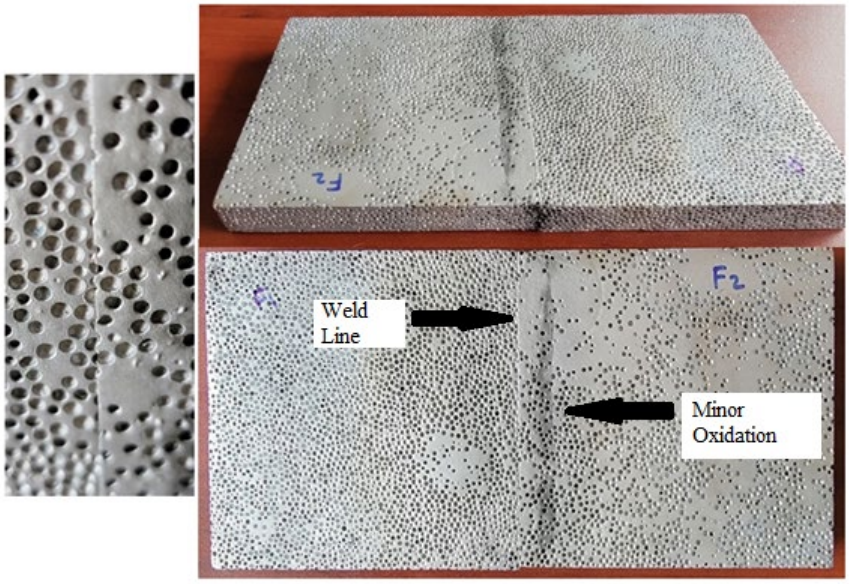

Fig. 2. Induction welded panels of steel-steel composite metal foam with an in-tact porous structure and surface free of defects. Some dark regions near the weld line indicate some degree of oxidation. Image courtesy of Advance Materials Manufacturing, LLC.

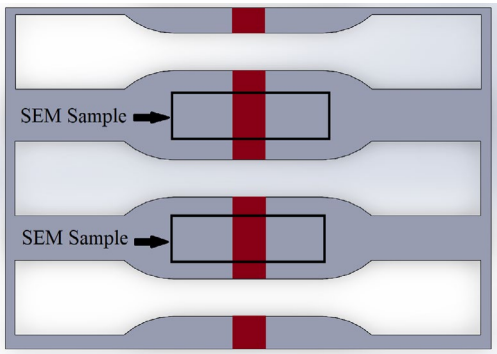

Fig. 3. Orientation of 3 tensile specimens along a pair of welded panels.

Specimens for microstructural analysis were sourced from the leftover material between the dog bone tensile specimen extraction sites then ground and polished using 180, 320, 600, 800, and 1200 grit Buehler SiC papers followed by 3 and 1µm Buehler MetaDi diamond suspensions, respectively. Both grinding and polishing processes took place on a Buehler AutoMet Powerhead 2 grinding and polishing station, with each grit being followed by ultrasonic cleaning in water then acetone before moving to the next grit to prevent cross contaminations. The welding area and its heat affected zone's microstructure was evaluated using a Scanning Electron Microscope (SEM).

Imaging was conducted using a Hitachi SU3500 SEM equipped with Electron Dispersive Spectroscopy (EDS) and Electron Backscatter Diffraction (EBSD).

2.2 Tensile testing

Tensile tests were executed in accordance with ASTM E8/E8M at a loading rate of 0.1mm/min, using a Q-Test Electromechanical Universal Testing Machine equipped with pneumatic grips and 20kip load capacity. Specimens failing at the weld line were set aside as outliers due to this type of failure representing an unsuitable bond. In turn, outliers were excluded from the data sets presented in this study.

3. Results and discussion

3.1 Preliminary structural observation

Preliminary SEM imaging of a cross-sectional S-S CMF strip extracted from the induction welded panels provided confirmation that the process was successful in joining the matrix between panels while effectively preserving the hollow spheres, with little distortion near the bonded interface. A broad view of a weld interface can be seen in Fig. 4 A) and B), showing a clean bond with only slight filling of the previously cut spheres being due to the forces imparted by thermal expansion while fixed in a vise during welding. The accompanying views in Fig. 4 C) and D) highlight higher magnification views of the fused matrix. The progressively higher magnification views of Fig. 4 are denoted sequentially by white squares showing their locations.

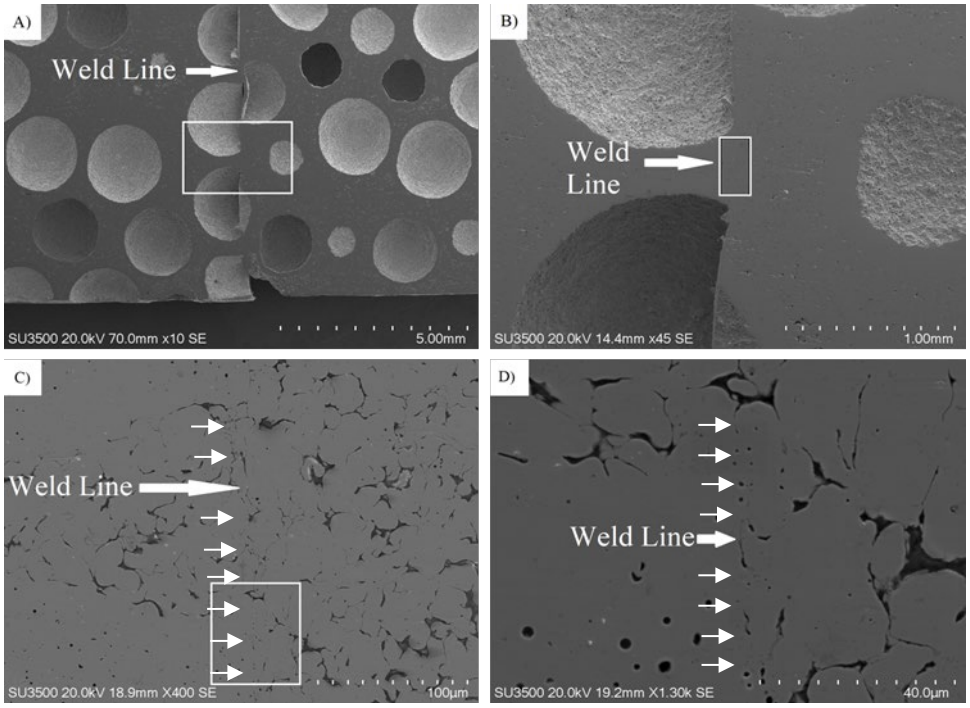

Fig. 4. A) A broad SEM image of the induction welded interface along S-S CMF panel, B) a magnified view highlighting a region of the weld, C) a further magnified view of the seamlessly welded matrix, and D) a final magnified image of the matrix, showing a near-seamless joint.

Rust was observed to be abundant throughout outlying tensile specimens produced in group 1, while being almost absent from group 2 specimens. This suggests the use of an argon welding environment fulfilled its desired role, as well as a possibility that the water-based flux used in group 1 may have contributed to oxidation. However, this effect requires further scrutiny to determine whether the flux is in fact problematic, or oxidation had alternatively resulted from sensitization of the heat affected zone (HAZ) due to precipitation of chromium carbide (Cr_3C_2). This effect is being studied and results will be reposted in future publication.

3.2 Mechanical behavior

Tensile tests revealed a wide range of performances across both sample groups, lending to the suspected impact of welding parameters on mechanical performance. Panel thickness and maximum temperature achieved during the welding process are the most important variables. Heat penetration is a documented limitation of induction welding [8], heavily influenced by phenomena known as skin effects. This occurs when the heating profile of a conductive material becomes distorted as induced Eddy current concentrates at the surface closest to the induction coil, resulting in a conical heating profile through the cross-section that narrows further from the coil. Depth of weld penetration in this case is inversely proportional to the welding frequency and magnetic permeability of the workpiece, rendering skin effects surmountable with iterative adjustment of the process parameters. [8] Implementation of the C-shaped coils was intended to prevent this, heating the workpiece from both top and bottom to optimize penetration of the heating profile, and appears to have been successful as obtained with the bonding of the 22.5mm thick S-S CMF panels (as shown in Table 1). However, Fig. 5 shows a steady decline in average ultimate tensile strength (UTS) of welds with increasing panel thickness., E1/E2, a 10.2mm thick panel, displayed an UTS of 63 MPa while 20 MPa was obtained with thicknesses approaching 25mm.. This trend suggests that thickness could be a limitation when induction welding S-S CMF.

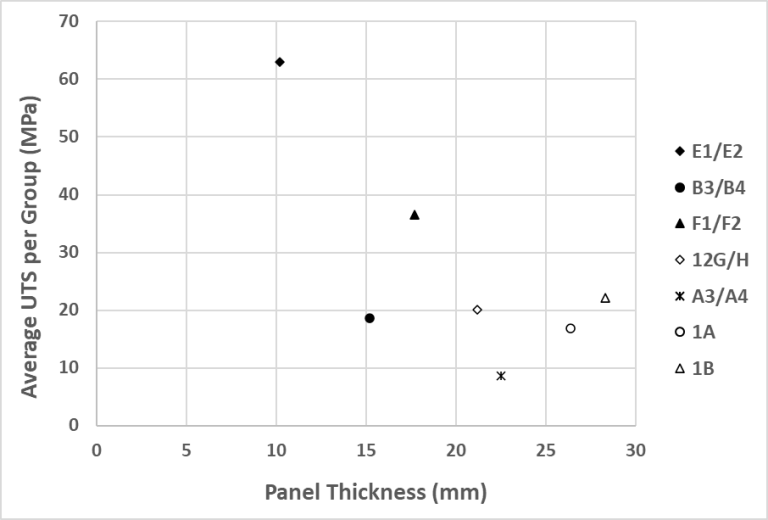

Fig. 5. Average ultimate tensile strength plotted against thickness of S-S CMF panels at the time of welding.

Contrary to the effect of thickness, rise in welding temperature appears to be directly related to the mechanical performance, as shown in Fig. 6. This behavior is expected as further liquefaction and solidification often intensify the degree of bonding between metals. A similar effect is present in the induction welded samples of this study with the panels essentially undergoing localized sintering at the bond interface. The sintering temperature of 316L stainless steel is known to dwell between 1100°C and 1300°C . [9] This correlates well with the observed tensile behavior, showing peak performance of 63 MPa paired with a welding temperature of 1220°C. While the current influences of thickness and temperature offer promising insight to the limitations and optimization of induction welding of S-S CMF, research is ongoing to isolate further influential factors such as coil size, welding power, preheating, and environment.

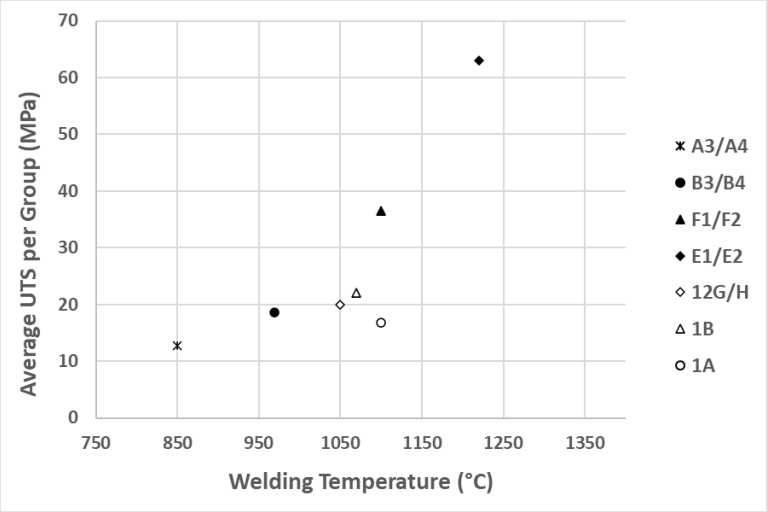

Fig. 6. Average ultimate tensile strength plotted against weld temperature of S-S CMF panels.

Conclusions

Observation and mechanical evaluation of S-S CMF panels joined through induction welding has granted a preliminary understanding of the viability of this process and its parameters. Broad SEM observations have shown that the process is overall successful in joining S-S CMF panels, with the matrix showing an indistinguishable interface and hollow steel spheres remaining nearly spherical with no distortion. Furthermore, welding temperatures comparable to sintering conditions were achieved, showing a clear benefit at higher temperatures, while panel thickness draws a clear limitation to the compatibility of induction welding of S-S CMF. Further investigation is ongoing to formulate decisive correlations between other process parameters and weld performance, though the present data appears promising.

Acknowledgements

The authors would like to express their gratitude to the United States Department of Transportation (DOT) for their financial support through the Pipeline and Hazardous Materials Safety Administration (PHMSA) award number PH957-20-0075. Additional gratitude is extended to Advanced Materials Manufacturing, LLC team of engineers and scientists to lead and conduct all induction welding works.

References

[1] J. Marx, A. Rabiei, Overview of Composite Metal Foams and Their Properties and Performance, Advanced Engineering Materials. 19 (2017) 1-13. https://doi.org/10.1002/adem.201600776

[2] Found on https://www.aar.org/wp-content/uploads/2021/02/AAR-Freight-Rail-Climate-Change-Fact-Sheet.pdf

[3] Found on https://tankcarresourcecenter.com/tankcar101/#1499693534177-d720d234-3972

[4] Found on https://www.tsb.gc.ca/eng/rapports-reports/rail/2013/r13d0054/r13d0054-r-es.html

[5] F. Garcìa-Moreno, Commercial Applications of Metal Foams: Their Properties and Production, Materials. 85 (2016) 1-27. https://doi.org/10.3390/ma9020085

[6] H.-P. Degischer, B. Kriszt, Handbook of Cellular Metals, WILEY-VCH Verlag GmbH, Weinheim, 2002. ISBN 3-527-60055-8

[7] B.P. Neville, A. Rabiei, Composite metal foams processed through powder metallurgy, Materials and Design 29 (2008) 388-396. https://doi.org/10.1016/j.matdes.2007.01.026

[8] T.J. Ahmed, D. Stavrov, H.E.N. Bersee, A. Beukers, Induction welding of thermoplastic composites - an overview, Composites: Part A. 37 (2006) 1638–1651. https://doi.org/10.1016/j.compositesa.2005.10.009

[9] P. Samal, J. Newkirk, Sintering of Stainless Steels, in: ASM Handbook Volume 7: Powder Metallurgy, AMS International, 2015, pp. 434-439. https://doi.org/10.31399/asm.hb.v07.9781627081757